AIAA JOURNAL
Vol. 39, No. 7, July 2001

Spray Generation from Turbulent Plane Water Wall Jets Discharging into Quiescent Air

T. Sarpkaya*
Naval Postgraduate School, Monterey, California 93943
and
C. F. Merrill†
Hydrodynamics/Hydroacoustic Technology Center, West Bethesda, Maryland 20817

This is an experimental investigation of the mutual interaction between the free surface structures (ligaments and drops) and the turbulent flow beneath them (high-speed, wall-bounded, supercritical free-surface flows or liquid wall jets, e.g., a bow sheet). Using tap water and water solutions of polymer additives, measurements were made with several high-speed imagers (250 to 8000 frames/s) and analyzed through the use of Optimas-MA software to quantify the characteristics of ligaments and drops. Four control parameters were considered: Reynolds, Froude, and Weber numbers and relative wall roughness, based on the initial jet thickness h_0, the mean exit velocity U_0, and the physical properties of air and tap water at 19°C. Sieved sand was used to obtain the desired relative wall roughness k/h_0. The Reynolds number ranged from 2.4×10^4 to 8.5×10^4, the Froude number from about 15 to 30, and the Weber number from 1500 to 7500. The distances to the start of the free-surface roughening, ligament formation, and drop generation were quantified. The characteristics of the ligaments and drops were evaluated for representative roughnesses through the use of Eulerian and Lagrangian measurements.

Nomenclature

C_d	=	drag coefficient
D	=	diameter
D_{dr}	=	drop diameter
D_{li}	=	ligament diameter
F	=	drag force on a ligament
Fr	=	Froude number, $U_0/\sqrt{(gh_0)}$
g	=	gravitational acceleration
h	=	local jet thickness
$\bar{h}$	=	local mean jet thickness
h_0	=	jet thickness at the edge of the plate
k	=	mean sand roughness height
k_w	=	wave number
k/h_0	=	relative wall roughness
L_{li}	=	ligament length
Re	=	Reynolds number, U_0h_0/ν
U_0	=	mean jet velocity at exit
u	=	streamwise velocity, $\bar{u} + u'$
$\bar{u}$	=	mean streamwise velocity
u'	=	fluctuating component of u
$\langle u' \rangle$	=	rms value of u' normalized by U_0
$\langle u'v' \rangle$	=	turbulent shear, $-u'v'/U_0^2$
v	=	vertical velocity, $\bar{v} + v'$
$\bar{v}$	=	mean vertical velocity
v_{rms}	=	rms value of v' normalized by U_0
v_{tip}	=	y component of a ligament's tip velocity
v'	=	fluctuating component of v
$\langle v' \rangle$	=	rms value of v' normalized by U_0
We	=	Weber number, $\rho U_0^2 h_0/\sigma$
x	=	axial distance along the plate
Y	=	$\sqrt{(We)}/Fr = h_0\sqrt{(\rho g/\sigma)}$
y	=	distance from the wall
Z	=	$\sqrt{(We)}/Re = \mu/(\rho D\sigma)^{1/2}$
δ	=	boundary-layer thickness
δ_t	=	turbulent boundary-layer thickness
δ_{XX}	=	uncertainty associated with (XX)
λ	=	wavelength
λ_i	=	wavelengths on a ligament
μ	=	dynamic viscosity of water
μ_a	=	dynamic viscosity of air
ν	=	kinematic viscosity of water
ρ	=	density of water
ρ_a	=	density of air
σ	=	surface tension

Presented as Paper 2000-0817 at the 38th Aerospace Sciences Meeting, Reno, NV, 10–13 January 2000; received 22 February 2000; revision received 5 February 2001; accepted for publication 8 February 2001.

*Distinguished Professor of Mechanical Engineering. Associate Fellow AIAA.

†Lieutenant Commander, U.S. Navy, Technical Director.

Introduction

THE formation of instabilities, wavelike structures, followed by ligaments, drops, and atomization, on relatively high-speed single or coaxial jets, with or without combustion, represents one of the many complex gas-liquid two-phase flows. The literature abounds with studies of atomization, spray generation, and related phenomena[1–5] partly because of their intrinsic interest and partly because of their practical applications in the breakup of circular liquid jets, combustion, irrigation, naval architecture (bow sheets, ship plunging, hydrodynamic stealthing), coating processes, chemical and/or nuclear technology, paper making, and ink-jet printing, just to name a few.

The main objectives of the present investigation were to delineate the primary characteristics of the free-surface structures (ligaments and drops) originating from plane turbulent liquid wall jets (water-into-air) along smooth and sand-roughened walls in terms of the governing parameters (Re, Fr, We, and k/h_0). The selection of the most appropriate ranges of these parameters was guided by the characteristics of bow sheets on full-scale destroyers. The water/air density ratio (here, $\rho/\rho_a \approx 820$) was not included among the governing parameters because it was previously shown[6–9] that the aerodynamic effects on free-surface structures are negligible for liquid/gas density ratios larger than about 500.

A critical review of the extensive literature has shown that the breakup of jets and sheets depends strongly on several internal/external influences[1–10] governing their creation and subsequent evolution. Some of these are the jet velocity profile and turbulence at the nozzle exit, gravity, surface tension, liquid-sheet geometry, wind or gas flow in coflowing jets as in cryogenic rocket engines,[11] combustion, roughness of the contact surface(s), the physical and thermodynamic states of both the liquid and gas, pressure fluctuations within and outside the jet, and acoustic excitation. Some of the

influencing parameters (e.g., nozzle shape) are beyond the experimental ability of the researcher to quantify.

One of the earliest analytical works examining the breakup of liquid jets is the linear analysis of Rayleigh.[12] He has shown that the maximum growth rate of an axisymmetric disturbance occurs at a wave number of $k_w = 0.697$. His results were later expanded by Weber[13] and Ohnesorge[14] to include the effects of viscosity. Squire[15] and, subsequently, Hagerty and Shea[16] carried out an inviscid flow analysis of the stability of a sheet of uniform thickness and found that instability occurs if the Weber number is greater than unity, i.e., when the inertia forces exceed the surface tension.

The stability of laminar plane sheet flows has been investigated by a number of researchers, starting with Brown[17] who has shown that to maintain a stable sheet there must be equilibrium between the inertia forces and the surface tension at the free surface. More recent studies (e.g., Luca[18]) dealt with the absolute or convective character of the instability and, in particular, with the determination of the critical Weber number corresponding to the breakup of falling capillary plane and round jets. A brief summary of these is given by Luca.[18] An inclined round jet is locally convectively unstable at every streamwise location, as shown by Yakubenko.[19]

In recent years the unravelling of the interaction of the turbulent boundary layer and small-scale free-surface deformations in channel and river flows has attracted considerable interest.[20–24] The existing measurements[20,23,24] are for very low-Froude-number flows ($Fr \ll 1$) where the free surface exhibits nothing more than irregular small fluctuations, in the order of millimeters in channels and centimeters in rivers. Moreover, their size relative to the depth of the flow is negligibly small and does not lead to a measurable interaction between the free-surface dynamics and the boundary layer extending to the bottom of the flow. The velocity measurements of Finley et al.[25] (with Preston tubes) in a thin turbulent water layer (over a smooth wall) with minimal free-surface distortions ($2 < Fr < 9$) have shown that the mean flow in the buffer and inner regions could be described by a power-low relationship. In the outer region, Finley et al.[25] claimed that the velocity profiles followed the usual log-law as if there were no free-surface disturbances. Binnie,[20] Benjamin,[21] Knuth,[22] and Sarpkaya and Neubert[23] have arrived at similar conclusions about the channel flows at very low Froude number.

Previous investigations[6–11,26,27] at sufficiently large Froude number have shown that the qualitative features of flows over spillways, plunge pools, open water waves, and annular liquid wall jets are quite similar. These observations and measurements have also suggested that turbulence generated near the leading edge of the wall propagates across the flow, reaches the air/water interface, and roughens the free surface (Fig. 1). This is followed by a region of turbulent breakup where a large number of ligaments emerge from the free surface. Some, but not all, of these ligaments give rise to one or more drops. Subsequently, the free-surface activity gradually subsides as a result of loss of momentum.

The question of how does the wall jet selectively accelerate and eject parcels of fluid across the liquid/air interface remains elusive for a number of reasons:

1) The stability analyses dealing with drop and spray formation from a liquid jet do not go beyond the nonlinear evolution after the onset of the jet breakup at the liquid-gas interface.[28]

2) Direct numerical simulations[29] are possible only at very small Reynolds numbers, particularly when the linear instability modes used as sources in the calculations are independent of viscosity, as noted by Freund et al.[29]

3) There has never been an experiment with a liquid wall jet, with ligaments and spray, where the distributions of mean as well as instantaneous flowfields and the complete Reynolds-stress tensor were measured at numerous sections downstream from the nozzle. This is caused by the extreme difficulty of making nonintrusive measurements (with laser Doppler anemometer, digital particle image velocimeter, and laser-induced fluorescence) in thin sheets of water because of unavoidable reflections from ligaments and water surface. The use of multiple digital coupled capacitive discharge (CDC) cameras and mirrors to resurrect the true images from the distorted vertical grid (the Scheimpflug condition) is both difficult and expensive.

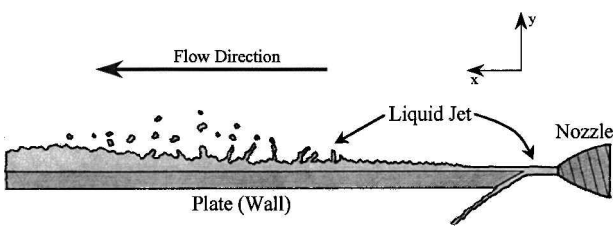

Fig. 1 Schematic drawing of a liquid wall jet discharging into air.

It appears that only a combination of 1) the evaluation of the kinematic and dynamic characteristics of ligaments and drops obtained through the use of flow visualization; 2) the measurement or the use of the existing measurements of the characteristics of the jet (at relatively smaller Fr); and 3) the use of the information gleaned from the semi-infinite boundary layers of wall-bounded flows and of liquid (gas) wall jets discharging into identical liquid (gas) will have to pave the way to numerical predictions and industrial applications.

The following is a brief summary of the existing information relevant to the present study:

1) There is little experimental and numerical work on the free-surface structures of high-speed free-surface flows.

2) The near-wall region of (semi-infinite) turbulent flows is characterized by randomly recurring high-speed sweeps and violent ejections.[30–32] The $u' - v'$ quadrant analysis[30,31] has confirmed that the sweeps occur in the fourth $(+u', -v')$ quadrant (Q4 event). Thus, they are wall-directed inrushes of higher than average downstream velocity. Ejections occur in the second $(-u', +v')$ quadrant (Q2 event). They are violent upward and backward moving parcels of fluid of lower than average downstream velocity.[33,34] In a liquid wall jet they could give rise to ligaments leaning mostly backward while moving forward with the stream.

3) The sweep phase is significant only near the wall, whereas the ejection phase is influential throughout most of the boundary layer.[33] The frequency of the ejection and sweep events increases with roughness.[35] Two or more ejections may join by dynamic and kinematic processes whose "focusing effect" may give rise to "bursts" of fluid that move away from the wall even at a higher velocity.[36–38] The relevance of such bursts to the generation of more energetic ligaments will be examined in more detail later.

4) The wall roughness greatly modifies[33,34,39] the low-speed streaks, high-speed sweeps, ejections and bursts, and a wide range of vortical structures (hairpin- and horseshoe-shaped vortices, and coherent structures). These changes render the mean flow three dimensional, particularly in the roughness sublayer, change the scale of the outer-flow motions, and give rise to higher energy ejections not existing in smooth wall flows.[33,34] Grass[33] was the first to show that as the size of roughness increases $\langle u' \rangle$ decreases near the wall and $\langle v' \rangle$ increases over the entire thickness of the boundary layer while still decreasing with y/δ. Grass[33] noted and Raupach[34] demonstrated that the ejected fluid behaves in a quasi-coherent fashion, moving almost vertically through the boundary layer. This is confirmed by Krogstad and Antonia,[39] who found that the frequency of the ejection and sweep events increases with roughness and that the influence of roughness is not confined to the near-wall region, as it is often assumed. It is important to emphasize that the data of Grass,[33] Raupach,[34] Krogstad and Antonia,[39] and van Oudheusden[40] have all shown that all turbulence quantities ($\langle u' \rangle$, $\langle v' \rangle$, and $\langle u'v' \rangle$) decrease with increasing y/δ. Thus, for a given k/h_0 the thinner of two jets of identical velocity U_0 should be expected to yield longer ligaments and larger drops.

5) In liquid wall jets the jet thickness increases as a result of loss of momentum to the wall. This is even more so in the case of sand-roughened walls. In either case the loss of momentum leads to the development of a retarded boundary layer with nonequilibrium turbulence. van Oudheusden,[40] working with a linearly retarded boundary layer along a flat plate, found that "Towards the end of the transition region the fluctuation levels in a large part of the boundary layer are significantly larger than in a fully developed turbulent boundary layer." He further noted that the "apparent overshoot in turbulence strength is also reflected in the measured distributions of mixing length and eddy viscosity in the outer region, which at the end of the transition region reach values of twice the normal levels."

6) An equally interesting and relevant issue is how the boundary layer responds to changes in surface roughness. Antonia and Luxton[41] showed that the inner boundary layer adjusts from a fully developed smooth profile to a rough profile within 20δ of the start of the roughened region. In the case of rough-to-smooth transition, Andreopoulos and Wood[42] found that the transition took over 55δ after the flow was exposed to a 150-mm length of roughness. Pimenta et al.[43] and Gibbings and Al-Shukr[44] concluded that the outer flow appears to have a fairly long "memory" of its upstream conditions and that roughness tends to shorten the length of the transition region. These finding are particularly relevant to liquid wall jets of relatively small depth where ligaments and drops come into existence shortly after turbulence intercepts the free surface.

7) With the exception of Grass,[33] all of the previous studies were limited to boundary-layer flows. Therefore, the question naturally arises as to how the free surface might affect the results just summarized. There is growing evidence that the free-surface structures (including ligaments and drops) are singular manifestations of ejections and bursting processes.[7,9–11,26,45–47] However, neither the turbulence structure of retarded boundary layers nor the kinematic and dynamic characteristics of ligaments and drops have been quantified for liquid wall jets discharging into air. As noted by Buttler Ellis et al.,[48] "The goal of being able to measure spray liquid properties and thereby determine spray quality cannot be achieved without a better understanding of the processes taking place at the interface between the spray liquid and air, and between the dispersed and continuous phases." From what has been seen and measured, it is evident that the internal flow structure of a liquid wall jet (water-into-air) is not the same as either that of a typical boundary layer or a typical air-into-air wall jet. The velocity profile in the latter case is largely influenced by the strong shear at the periphery of the jet (in addition to the distance from the nozzle, velocity profile and turbulence contained within the jet at birth).

The present work, motivated by the preceding discussion, is aimed at the quantification of the mutual interaction between the surface structures and the turbulent flow beneath them in high-speed plane water jets discharging into air. The qualitative and quantitative description of the characteristics of ligaments and drops through observations and measurements in Eulerian and Lagrangian systems constitute the primary objectives of the investigation. The establishment of approximate best-fit correlations between representative geometric characteristics of the surface structures, such as the location of the onset of turbulent breakup or the Sauter mean diameter of drops in terms of the Weber number (to some power) was not one of the objectives of the investigation.

The preliminary reports of this study, emphasizing flow visualization and the characteristics of the surface structures, were presented by Sarpkaya and Merrill.[47,49] The remainder of the paper begins with a detailed description of the apparatus and procedures. This is followed by a discussion of the results through the use of histograms, mean velocities, and flow visualization. Finally, the key findings are summarized.

Apparatus and Procedures

Nozzle/Tunnel/Test Plates

The first test facility consisted of a two-dimensional nozzle of aspect ratio of 32 and contraction ratio of 13.9 (Figs. 2 and 3). It was fabricated out of two solid blocks of aluminum using the wire electron discharge machining process, and its surfaces were covered with a smooth polymer coating to prevent corrosion. It was attached to a large U-shaped water tunnel[50,51] (10 m wide and 7.5 m high) at a suitable location along one of its two vertical towers (Fig. 4). The upstream face of the nozzle (facing the tunnel wall) was carefully streamlined so as to provide a smooth entrance into the nozzle as shown in Fig. 5. It was known[52,53] early on that the nozzle design has a significant impact on the characteristics of the resulting jet and that data from various sources cannot be compared on the basis of the quantifiable governing parameters alone. The nozzle chosen (Figs. 2 and 3) embodies all of the past recommendations[52,53] (e.g., a gradual geometric transition, continued acceleration, earlier transition on the walls, and a thinner turbulent boundary layer).

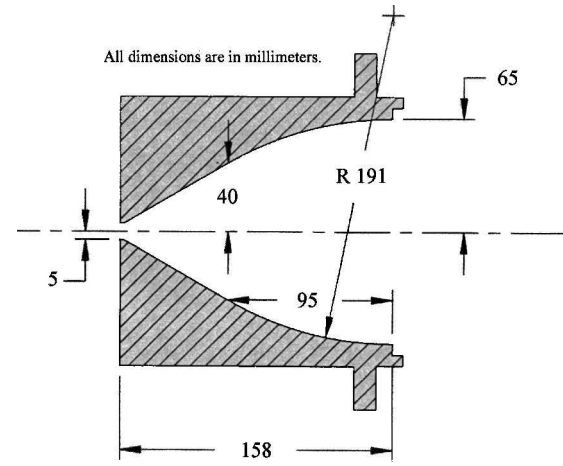

Fig. 2 Two-dimensional nozzle (aspect ratio = 32).

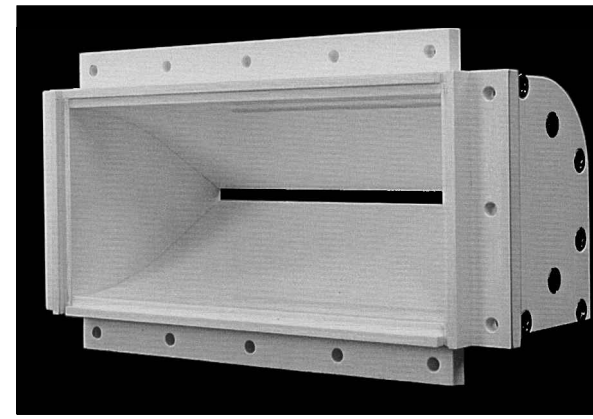

Fig. 3 Photograph of the nozzle shown in Fig. 2.

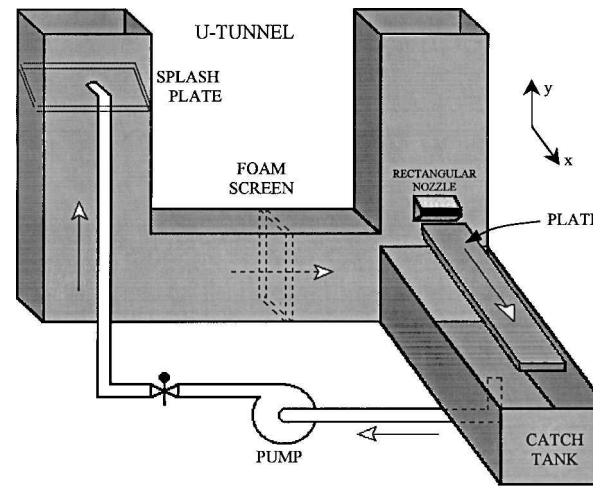

Fig. 4 U-shaped water tunnel, nozzle, test plate, and flowpath.

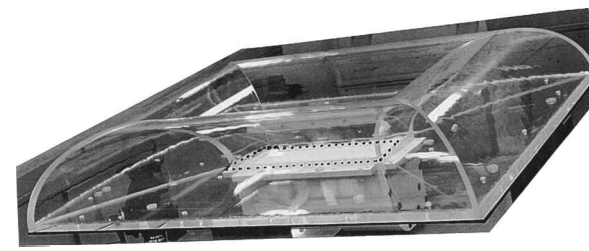

Fig. 5 Photograph of the upstream view of the nozzle.

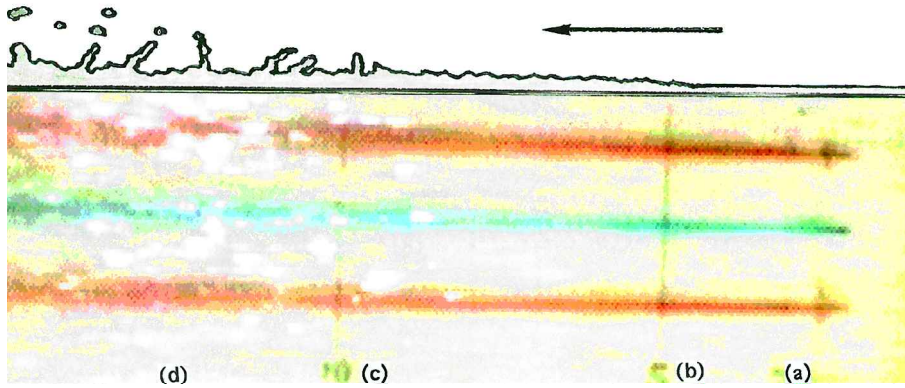

Fig. 6 Schematic of the side view of the jet and the top view of the plate and dye lines: a) inception of transition to turbulence on the wall and the end of molecular diffusion of the dye, b) interception of turbulence with the free surface, c) beginning of the ligament formation region, and d) region of ligaments and drops.

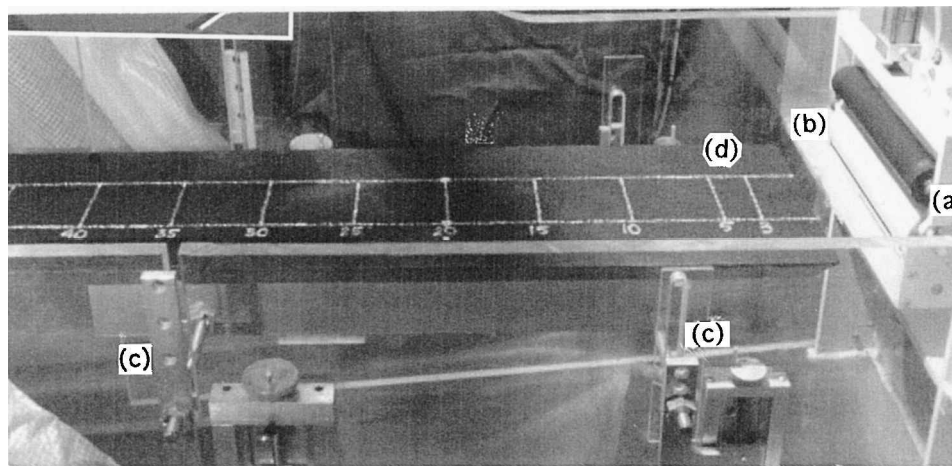

Fig. 7 Photograph of the test plate installed in the wall-jet apparatus: a) roller gate, b) nozzle exit, c) plate elevation controls, and d) test plate.

The discharge from the nozzle was collected in a trough and then pumped back into the U-shaped tunnel. The return flow discharged onto a large inclined plate along the top of the opposite tower of the U tunnel to avoid direct impact on the water surface and thereby minimize the disturbances to the fluid inside the tunnel. There was a distance of about 10 m between the return line and the nozzle. To further reinforce quiet flow conditions inside the tunnel, a foam divider, sandwiched between two heavy wire screens, was inserted near the midlength of the horizontal section of the tunnel. These precautions have indeed ensured that the flow entering into the nozzle was free from disturbances, as verified by flow visualization using food coloring (Fig. 6). With this arrangement it was easy to maintain constant jet velocities from 3 to 6.5 m/s indefinitely. The use of a nearly ideal nozzle, long observation and measurement times, and reliance on high-speed imagers made the entire apparatus particularly unique for the investigation under consideration. The additional advantages of the system were the relative ease with which the test plates (smooth or rough) could be interchanged, bodies of special interest could be mounted, and the flow could be illuminated and photographed.

The basic test plate was a 33-cm-wide and 183-cm-long Plexiglas® plate, mounted horizontally and rigidly on vertically adjustable supports (Fig. 7). The upstream edge of each plate was beveled with a sharp edge at an angle of 30 deg from the horizontal. The elevation of the sharp edge of the horizontal plate was positioned carefully so as to capture only the top 5–6.5 mm of the 8.5-mm jet. In a subsequent series of experiments, the nozzle height was increased from 10 to 20 mm to change the range of the governing parameters.

Some plates were sand-roughened carefully to achieve the desired relative mean roughness height of k/h_0 (from 0.01 to 0.13). For this purpose Monterey Beach sand was sieved numerous times with several sieves to obtain the desired roughness and applied uniformly on the test plates with an air-drying epoxy paint. The resulting surfaces were carefully examined through the use of a scanning electron microscope. Figure 8 shows a sample of many such photographs with a 75 magnification. The postexamination of the cross section of one of the plates has shown that the thickness of the epoxy paint was about 0.01 mm. The average height of the meniscus of the paint at the bottom of the grains was about 0.03 mm. The test conditions are summarized in Table 1.

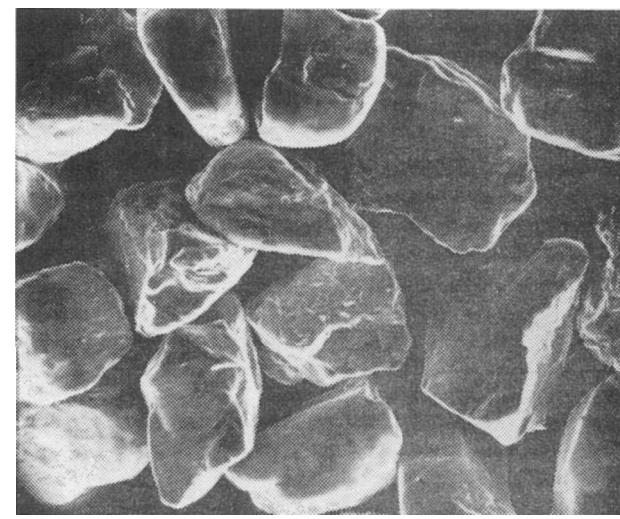

Fig. 8 Scanning electron microscope photographs of sand-roughened plate (k = 0.35 mm, magnification = 75).

Table 1 Summary of test conditions

Parameter	Range
h_0, mm	5.4–15
k, mm (sieved sand)	0.13–0.33
k/h_0	0.02–0.13
Liquid	Water
U_0, m/s (facility range)	3–6.5
U_0 (for the data reported herein)	6.2 m/s
ρ/ρ_a	820
$Fr = U_0/\sqrt{(gh_0)}$	15–30
$Re = U_0 h_0/\nu$	24,000–85,000
$We = \rho U_0^2 h_0/\sigma$	1,500–7,500

Recirculating Water Tunnel

The second test facility consisted of a high-speed free-surface water tunnel (about 8 m^3) and used primarily for the acquisition of velocity and vorticity data through the use of a digital particle image velocimeter (DPIV) system. The tunnel is a slightly modified version of the so-called Göttingen tunnel,[54] currently located at the National Research Council of Canada. The open test section is 50 cm wide, 50 cm deep, and about 6 m long and has large Plexiglas® windows on all three faces. It spans the gap between the 4-to-1 contraction and the return leg duct. When necessary, removable plates can be used to close the top of the working section. During the off-test periods, a small pump continuously filtered the tunnel water through a microfiltration system to remove rust and other suspended fine particles, down to about 10 μm, from the water. The wall jet was created by placing an adjustable streamlined gate at the upstream end of the test section where the closed section joined the open section. Smooth and sand-roughened Plexiglas plates were placed at the bottom of the test section. The jet velocities of about 6 m/s were easily achieved through the use of a 50-Hp pump.

Jet/Plate Interaction

The jet exited from the nozzle (Figs. 6 and 7) upon the removal of a cylindrical gate (through the use of a pneumatically controlled rotating cylinder). After a short flight (about 80 mm) the desired thickness of the jet was captured by the horizontal test plate (Figs. 1 and 7). The initial thickness of the jet on the plate h_0 was measured using 1) a point gauge and 2) the change in the conductivity of a platinum wire immersed in the jet. The wire was frequently calibrated by immersion in known water depths, using water extracted from the jet at the time of the calibration. The preceding methods had an accuracy of $\pm$ 0.1 mm. A third and a very quick method was the use of a 3-mm-wide and 37-mm-long razor blade (with 0.5-mm divisions). It was immersed into the jet at zero angle of attack without violating the state of the free surface. This method gave the jet thickness within $\pm$0.5 mm. The jet thickness was varied by raising and lowering the horizontally mounted test plate through the use of four large gears (Fig. 7). The slope of the test plate in all directions was measured with a digital inclinometer, accurate to 0.01 deg.

The jet surface had a fine-grained texture on emergence caused by the evolving shear layer, as previously observed by Hoyt and Taylor.[8] The grainy structure disappeared only at relatively low velocities ($Fr < 1$), and the jet had a smooth glassy surface, as if it were frozen. In either case, however, the jet was nonturbulent by the time it reached the edge of the plate. Figure 6 shows three dye filaments, introduced from 0.8-mm dye ports along a line about 50 mm from the leading edge of the plate. The dye filaments underwent molecular diffusion for about 40 mm (Fig. 6). Then, they began to diffuse rapidly, indicating that the jet has quickly transitioned to turbulence (within 90 mm from the edge of the plate). Only at relatively small Froude numbers ($Fr < 1$) did the growing laminar boundary layer reach the free surface first before eventually becoming turbulent. For Froude numbers of interest to this study ($Fr > 15$), the laminar region of the boundary layer was relatively inconsequential as shown in Fig. 6. Then, turbulence intercepted the free surface at some point downstream (referred to hereafter simply as the turbulence interception point or TIP). All other free-surface events (ligaments, drops) occurred farther downstream from the TIP.

It became clear during the evaluation of data that it would be desirable to track the evolution of a given ligament. This would enable one to obtain sharper images and to trace the evolutionary history of the ligament. For this purpose a parallel railing system was constructed, and a camera was mounted on the carriage (Fig. 9). The carriage was accelerated to a nearly constant speed through the use of a suitable number of weights and a pulley system. When the system was ready for a new test, a switch was actuated to release the load and thereby to move the camera at desired speeds. This mechanism provided as many as 75 frames, separated by 1-ms intervals. Thus, it was possible to obtain displacement, velocity, and acceleration information from a selected number of images. Figure 10 shows a sequence of 7 of 38 frames (at 5-ms intervals). The life of this particular ligament, from birth to reduction to a small disturbance, was about 193 ms.

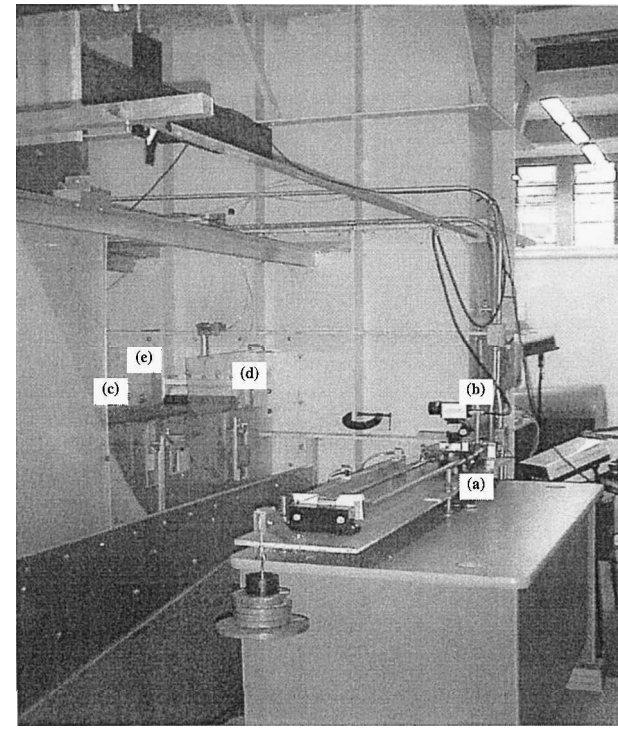

Fig. 9 Equipment for Lagrangian observations: a) parallel railing, b) camera, c) test plate, d) roller gate, and e) position of infrared laser.

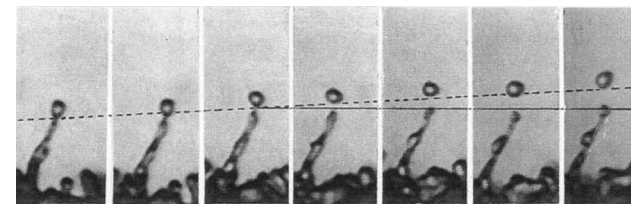

Fig. 10 Sequence of 7 frames of 38 (at 5-ms intervals). The life of this particular ligament, from emergence to final reduction to a small disturbance, was about 193 ms.

Instrumentation and Evaluation

Instrumentation for both facilities consisted of several high-speed cameras with frame rates from 250 to 8000 frames/s (with shutter speeds from 1/250 to 1/10,000 s) and a DPIV system. The recordings of the jet surface, ligaments, drops, and the scales inscribed on the plate were made along the jet (within a 183-cm-long and 30-mm-wide centrally located strip, along the longitudinal axis of the plate) through the use of proper lenses and back and front lighting. This ensured that a single ligament or a drop could be tracked during its lifetime (100–300 ms), from its creation to its return to the body of the jet, without being obscured by the shadows of ligaments in neighboring planes.

The video images were first carefully reviewed to identify a large number of representative ligaments (with or without drops) whose motion could be traced with little or no ambiguity. The diameter,

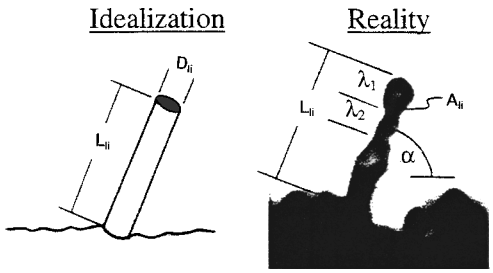

Fig. 11 Diagram showing the simplification of the ligament characteristics for statistical analysis.

volume, tip velocity, and lifespan of ligaments, the wave number of the axisymmetric disturbances, time of drop formation, drop size and velocity, free surface velocity, the temporal mean value of the local jet thickness, in addition to the distances to the region of transition and free-surface roughening, to the region of surface distortions and ligaments, and to the region of ligaments and drops were evaluated through the use of a suitable software (Optimas-MA). The characteristic diameter of a ligament was evaluated by drawing a contour around the ligament (Fig. 11) and automatically evaluating the enclosed area above the free surface and, from there, the characteristic diameter and volume. High-speed video images taken directly from above the jet as well as the visual observations with a high-speed stroboscope have shown that well-defined ligaments were almost always nearly axisymmetric.

Uncertainty Analysis

For the quantitative data provided in this research, the uncertainty was determined at a 95% confidence interval. The biases associated with the measurements in this analysis appeared inconsequential relative to the random variance of the data and the precision level of the individual measurements. Therefore, the data variance and the number of observations dictated the mean-value uncertainty, whereas individual measurement uncertainties were precision controlled. To minimize the uncertainty, it was important to record as many observations as reasonably possible and to arrange the measuring equipment to maximize its accuracy. Because this was the first investigation into the physics of this type of ligament and drop formation process, there was no a priori knowledge of the various parameter distributions. Hence, the number of observations of a given feature was kept greater than 30 so that the implicit analytical assumption of a Gaussian distribution could not introduce significant error into the mean-value confidence intervals.[55]

The surface characteristics (i.e., ligaments and drops) of the liquid wall jet were recorded on videotape using a high-speed imager positioned along side of the jet. The videotape was then reviewed to find ligaments and drops that could be analyzed with a reasonable degree of accuracy. The criteria used to make this determination were the following: the base of the ligament is clearly discernible, the ligament behaves in an axisymmetric manner, the entire ligament and the drops that it produces are unobstructed by other surface structures, the ligament and drops are in focus, the drops are very nearly circular in every image where the drop areas are measured, and the drops and ligaments can be measured in at least three sequential images.

The images of ligaments and drops meeting the preceding criteria were digitized and then analyzed on a PC using the Optimas-MA software. Based on the length scale prescribed and the time between the images, Optimas calculated the two-dimensional areas, angles, lengths, centroids, and relative positions, as well as velocities and accelerations of the various items. After the image analysis was completed, Optimas recorded the selected values to a text file or a Microsoft Excel spreadsheet. The same images of the ligaments and drops were then independently subjected to the same analysis by another person through the use of the same software.

The uncertainty analysis performed for this study used the constant odds (rms) formula and 95% confidence level uncertainty intervals as recommended by Moffat.[56] Adding some complexity to the calculations was the fact that some of the parameters requiring uncertainty analysis were not measured directly. For example, the calculation of the drop diameter was based on its measured cross-sectional area. Nonetheless, the primary uncertainties associated with this analysis were a function of the overall imaging system characteristics and the user's ability to accurately identify the free surface features using the Optimas software.

For the items measured directly the following uncertainties have been identified:

1) Object definition: The uncertainty associated with the user's ability to outline the exact shape of an object (estimated value = $\delta_{OBJ} = 0.14$ mm).

2) Object not at the focal plane ($\delta_{FO} = 0.04$).

3) Lens distortion ($\delta_{LS} \approx 0$).

4) Length-scale calibration error ($\delta_{LE} = 0.0089$).

5) Optimas area calculation approximation ($\delta_{AR} = 0.0025$).

6) Observer interpretation: Different individuals will define an object somewhat differently. The uncertainty of this factor was determined for each measurement by having two individuals independently analyze the identical image sequences (average $\delta_{OI} = 0.07$).

The use of the foregoing led to the following experimental uncertainties (95% confidence): drop size (<10%), ligament diameter (<17%), ligament length (<7.5%), x component of the drop velocity (<17%), y component of the drop velocity (<25%), jet velocity (<3.5%), jet thickness on smooth and rough plates (<4.8%), disturbance wavelength (<25%), and for the local mean jet thickness (at all locations) (<5.7%).

Results and Discussion

This was the first investigation of spatially developing high-speed liquid wall jets over artificially roughened plane boundaries. The highly disturbed nature of the free surface, insufficiency of the existing tools for precise measurements, the smallness of the jet thickness, the nonequilibrium nature of the flow, and the fact that the most important events transpire in less than about 300 ms, over a distance of about 1.5 m, rendered the investigation extremely difficult. Clearly, the acquisition of data over the entire range of parameters that would be needed for the development of a comprehensive theory would require new tools and considerable time. The establishment of approximate best-fit correlations between the representative

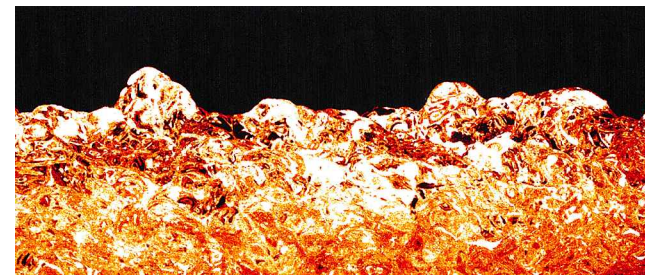

Fig. 12 DPIV image of a roughened free surface. The flow is from left to right.

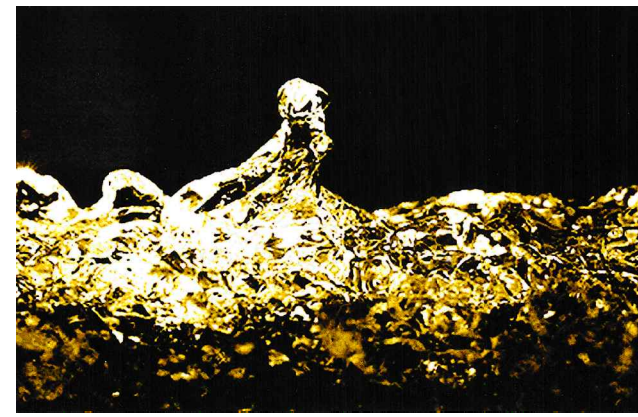

Fig. 13 DPIV image of the jet in the region of surface distortions and/or ligaments (exposure 7 ns). The flow is from left to right.

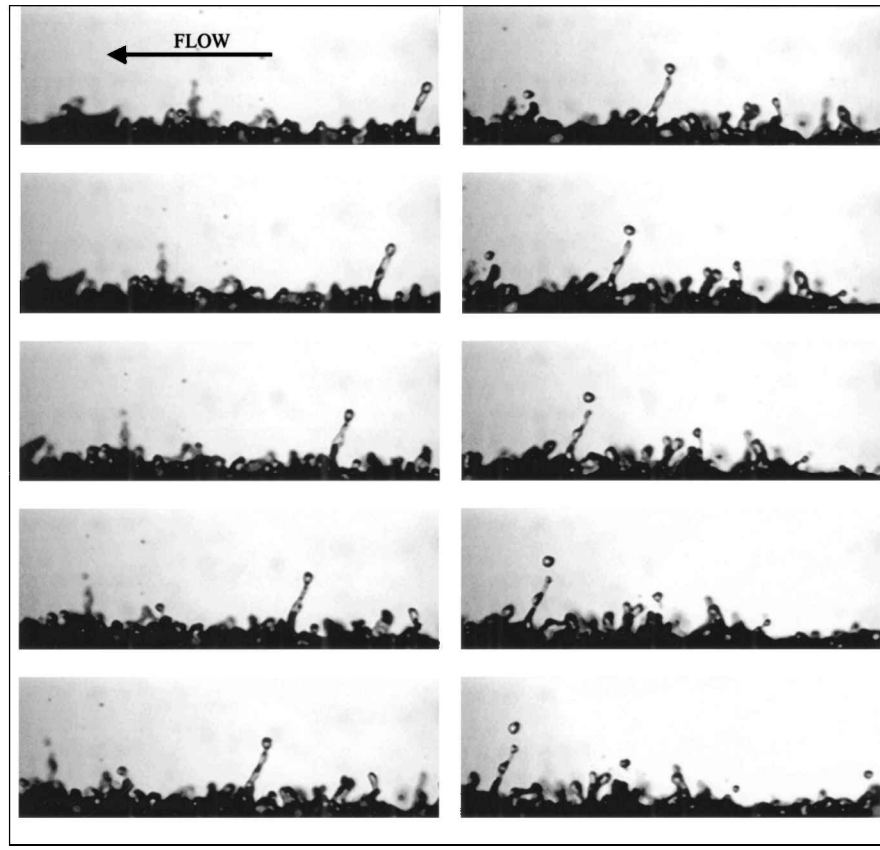

Fig. 14 Sequence of 10 frames (at 5-ms intervals from top to bottom and from right to left) in the region of ligaments and drops. The life of the longest ligament, from emergence to final reduction to a small disturbance, was about 193 ms.

mean geometric characteristics of surface structures and the Weber number can be useful for industrial applications, but such an effort is not expected to enhance the understanding of the physics of the phenomenon and the development of numerical simulations.

Evolution of the Free Surface

Observations and nonintrusive measurements have shown that the free surface evolves in four distinct stages: 1) the region of transition and roughness in which the turbulent boundary layer reaches the free surface and measurably roughens it but there are not yet any ligaments (Figs. 6 and 12); 2) the region of surface distortions and ligaments in which there are large surface distortions and/or ligaments but no drop formation (Fig. 13); 3) the region of numerous ligaments and drops in which there are ligaments giving birth to one or more drops as well as ligaments with no drops (Fig. 14); and, finally, 4) the region of decreasing activity in which surface structures gradually subside because the jet has lost most of its momentum to both the wall and the free surface during its first three stages. This is also the stage where most of the drops plunge back into the jet (Fig. 15).

The determination of the distance from the edge of the plate to the TIP through analysis and/or measurements is not a meaningful exercise because the gradual nature of surface transitioning defies precise position identification, as in all "transitions" in fluid motion. This is notwithstanding the fact that numerous efforts have been made in the past to quantify it. Just to mention a few of the more recent and easily accessible contributions, Phinney[26] and McCarthy and Malloy[27] observed that the breakup of the liquid jet was affected by the turbulence at the jet exit. More recently, Dai et al.[9] provided some approximate correlations in a narrow range of Reynolds numbers "assuming a 1/7th velocity distribution power law" for annular liquid wall jets flowing over thin smooth rods equipped with a tripping wire. A similar analysis is not presented here for a number of reasons: 1) the position of the TIP is very sensitive to facility-dependent parameters (entrance conditions, nozzle geometry, roughness of the plate, initial turbulence and swirl); 2) the parameters characterizing

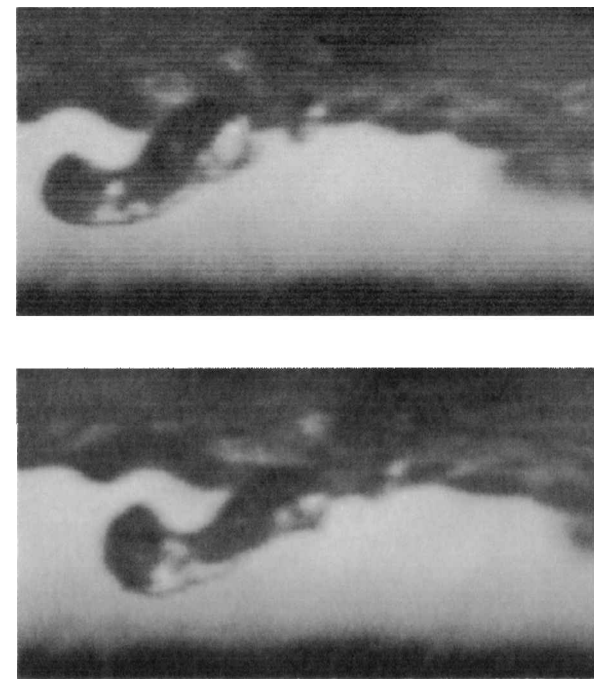

Fig. 15 Plunging of a drop back into the jet. The frames are 1 ms apart, and the flow is from the left to the right.

the initial state of the flow (velocity distribution, free shear layers), and the evolution of the nonequilibrium turbulence between a deformable free surface and a rigid wall are not sufficiently understood; 3) the smooth plates do not lead to drop formation in any region of the plate within the range of the parameters encountered; 4) the transition on sand-roughened plates is a much more complex problem.[57] It can be calculated numerically and only approximately through the use of suitable velocity profiles appropriate to rough-wall boundary

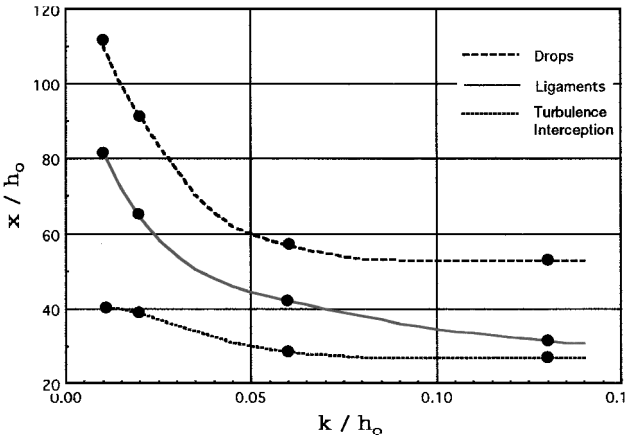

Fig. 16 Distances to turbulence interception with the free surface, ligament formation, and drop generation.

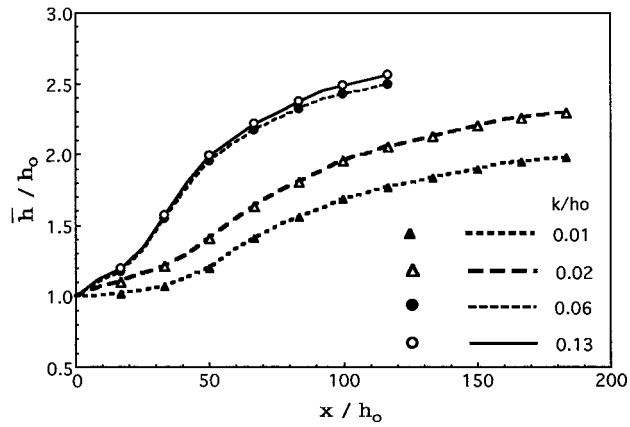

Fig. 17 Normalized mean jet thicknes as a function of the normalized distance from the tip of the test plate.

layers.[57] According to Davies,[58] van der Hegge-Zijnen[59] devised an approximate equation for the turbulent boundary layer δ_t over a rough wall where $\delta_t = 0.26k(x/k)^{2/3}$. As pointed out by Davies,[58] δ_t is no longer a function of U_0. Substituting $\bar{h}$ for δ_t, one finds that the predicted distance to the TIP is 25–100% larger than that measured. The present observations with rough walls have shown that (Fig. 16) turbulence begins almost immediately after the start of the plate and reaches the free surface within $25h_0$ to $40h_0$, depending on k/h_0 (from 0.01 to 0.13). However, the distances to the TIP, to the ligament formation, and to the drop generation nearly cease to depend on roughness beyond some minimum value of k/h_0 (about 0.06). The temporal mean jet thickness (see both Figs. 16 and 17) increases by 15–50% from the leading edge of the plate to the TIP, with an average increase of about 40% within the range of the parameters encountered. The mean value of $\bar{h}/h_0$ is found to be 1.4 ± 0.2 at the TIP, 1.7 ± 0.3 at the start of the ligament formation, and 2 ± 0.25 at the beginning of the drop generation region. These average values are for all of the tests performed in this investigation each test is uniquely defined by k/h_0 and Fr or by k/h_0 and We because the fluid properties and U_0 were maintained constant.

Ligaments and Drops

Although the sizes of all drops recorded were measured, the present discussion will focus on those formed at the ligament tips in the region of ligaments and drops. As noted here and in other studies,[60] a majority of the ligaments give birth to only one drop at the ligament tip. Even for those that form more than one, the "tip drop" is almost always the first and the largest. The few drops not produced by this process were very small ($D_{dr} \sim 0.25$ mm), and their formation appeared to be similar in nature to that of free-surface jetting described by Rein.[45]

There are a number of additional measurements that could have been made from the digitized free-surface images. However, here the analysis is directed toward those measurements that appeared to be the best indicators of the ligament formation and drop generation. Those indicators are the drop size and the length, diameter, velocity, and the acceleration of the ligament. It is believed that their measurements give the clearest possible indication of the events causing the drop formation, as well as the energy associated with their vertical motion. Histograms, computed over 8800 realizations, are used to compare and contrast the results of a large number of tests.

Figures 18–20 show the number frequency (probability density function) of D_{dr}/h_0, D_{li}/h_0, and L_{li}/h_0 for two Froude numbers (achieved by varying h_0 while maintaining U_0 constant). The

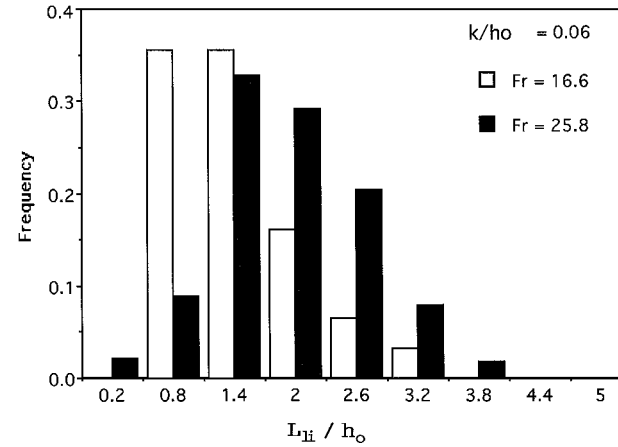

Fig. 18 Comparison of normalized ligament lengths for two Froude numbers ($k_0/h_0 = 0.06$).

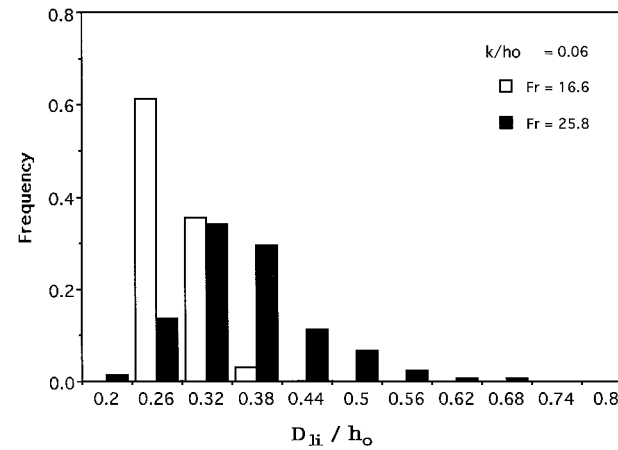

Fig. 19 Comparison of normalized ligament diameters for two Froude numbers ($k_0/h_0 = 0.06$).

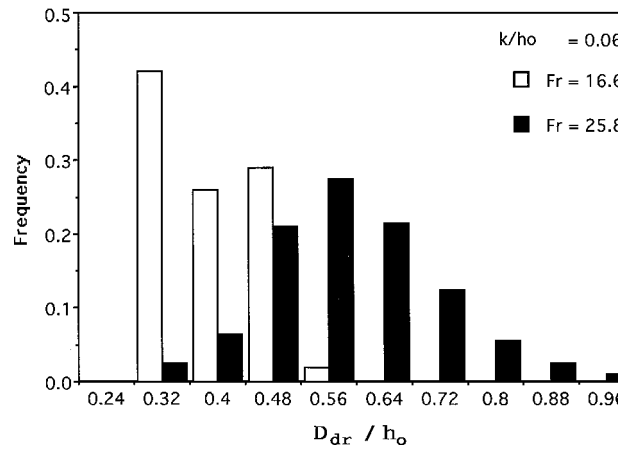

Fig. 20 Comparison of normalized drop diameters for two Froude numbers ($k_0/h_0 = 0.06$).

results are in conformity with the expectations based on the infinite boundary-layer data,[33,34,39,40] which have shown that the dimensionless measures of turbulence intensity decrease with distance from the boundary. Thus, wall jets of smaller Froude number (larger jet thickness for the same ambient velocity U_0) should give rise to smaller drops and shorter and thinner ligaments in narrower ranges of the ligament length and diameter, all within a relatively narrow range of Weber numbers. However, their frequency is somewhat larger. This is not surprising in view of the fact that the ejection events in the outer region of a boundary layer have higher frequencies and less pronounced peaks.[32–34] Figures 18–20 also show that the ligament lengths are almost always larger (as much as four times) than the initial jet thickness. However, the ligament and drop diameters are always smaller than h_0. Thus, it appears that ligaments can be longer than the larger eddies spanning the local thickness of the jet, but the drops are a small fraction (the tip region) of ligaments and are not expected to exceed h_0.

Figures 21–23 show the frequencies of D_{dr}/h_0, D_{li}/h_0, L_{li}/h_0, and L_{li}/D_{li} (ligament slenderness ratio) for four roughnesses for $We = 3000$ ($Fr = 26$). Apparently, D_{dr}/h_0 increases with increasing roughness, and its frequency distribution broadens out. The distributions of the ligament diameter (Fig. 22) and length (Fig. 23) exhibit a more apparent skew relative to that of the drop diameter. As the relative roughness increases, the distributions broaden and shift to the right, i.e., the mean values of D_{dr}/h_0, D_{li}/h_0, L_{li}/h_0, and L_{li}/D_{li} increase with increasing roughness.

The data shown in Figs. 21–23 are supported by the findings of Grass,[33] Raupach,[34] and Krogstad and Antonia,[39] who have shown that as the size of roughness increases $\langle v' \rangle$ increases over the entire thickness of the boundary layer, the ejected fluid moves almost vertically through the boundary layer, and the frequency of the ejection

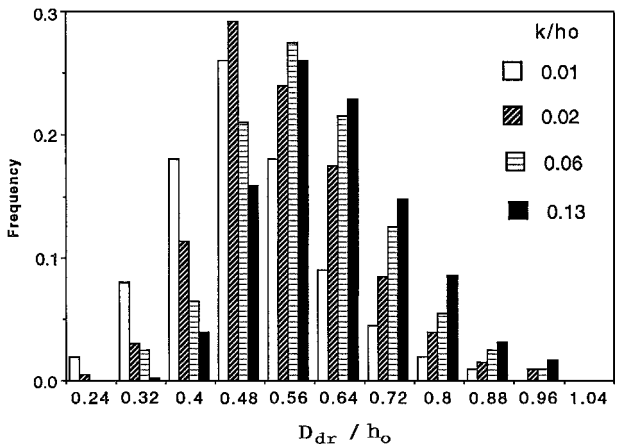

Fig. 21 Disturbance of normalized drop diameter as a function of relative roughness ($Fr = 26$).

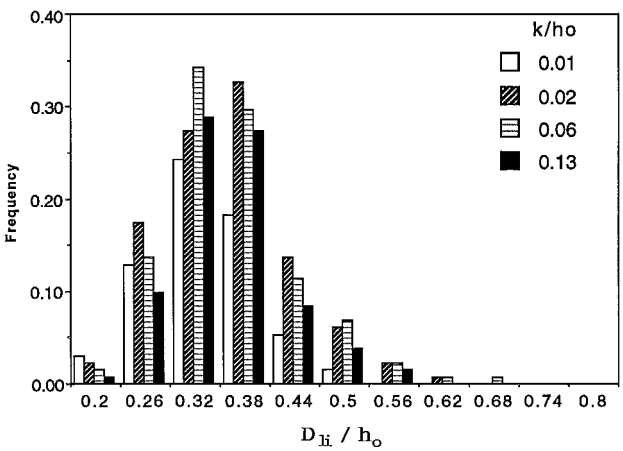

Fig. 22 Distribution of normalized ligament diameter as a function of relative roughness ($Fr = 26$).

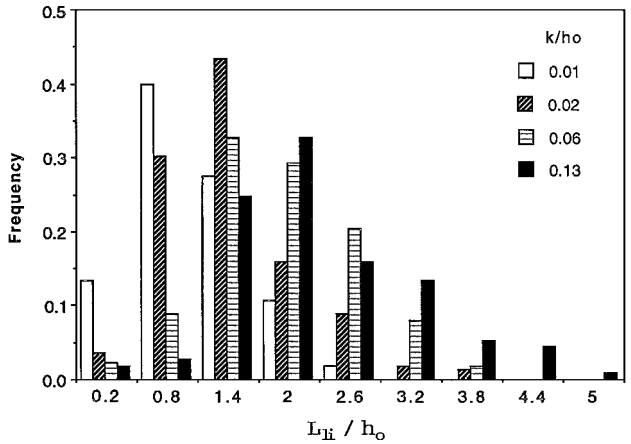

Fig. 23 Distribution of normalized ligament length as a function of relative roughness ($Fr = 26$).

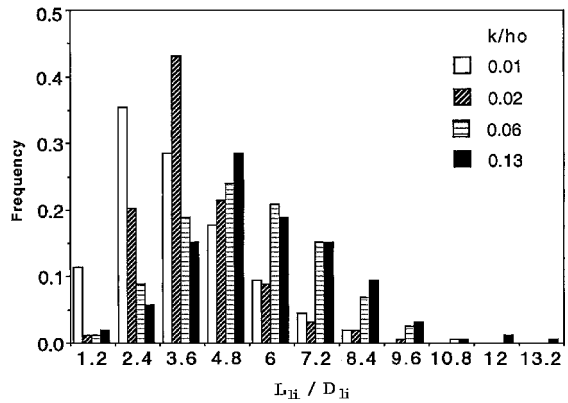

Fig. 24 Distribution of normalized ligament slenderness as a function of relative roughness ($Fr = 26$).

and sweep events increases. The data at smaller Froude numbers are not shown here for sake of brevity. However, they too support the arguments presented in connection with Figs. 18–26.

A series of experiments was carried out to change the character of turbulence in the jet through the use of a polymer (here Polyox-301) and three relative roughnesses. It has been shown by a number of investigators[6,7,61] that for concentrations less than 20 ppm the behavior of the polymer solutions is similar to that of water and yet their effect on drag reduction in tubes is indeed surprisingly large. A solution of Polyox (10 ppm) was carefully prepared and introduced into the tunnel. The details are given in Sarpkaya et al.[62] and will not be repeated here. The experiments at $Fr = 26$ ($We = 3000$) have shown that the long-chain polymer solution dramatically reduces the size of the ligaments (Fig. 25), confirming the earlier observations of Hoyt and Taylor[6,7] and the fact that the free-surface structures are created and controlled by the turbulence beneath the surface, not by free-surface waves. Anything that controls the intensity of turbulence (in our case, the wall roughness and the polymer additive) can and will control the size and frequency of the surface structures. No figures are presented on drop characteristics because no drops were created at $Fr = 26$ ($We = 3000$) with 10 ppm Polyox in water.

Lagrangian Observations

In the following the characteristics of single ligaments are described. Unlike the earlier cases where many ligaments are observed from a stationary platform, here only single ligaments and their evolution are traced as a function of time. The pictorial view (7 frames of 38) of the midlife period of a ligament and the pinch-off of drops were already introduced in Fig. 10. The vertical displacement and velocity of the tip and centroid of such ligaments were evaluated as a function of time.

It is seen (Figs. 10 and 14) that the ligaments under observation are inclined slightly backward, have several waves along their

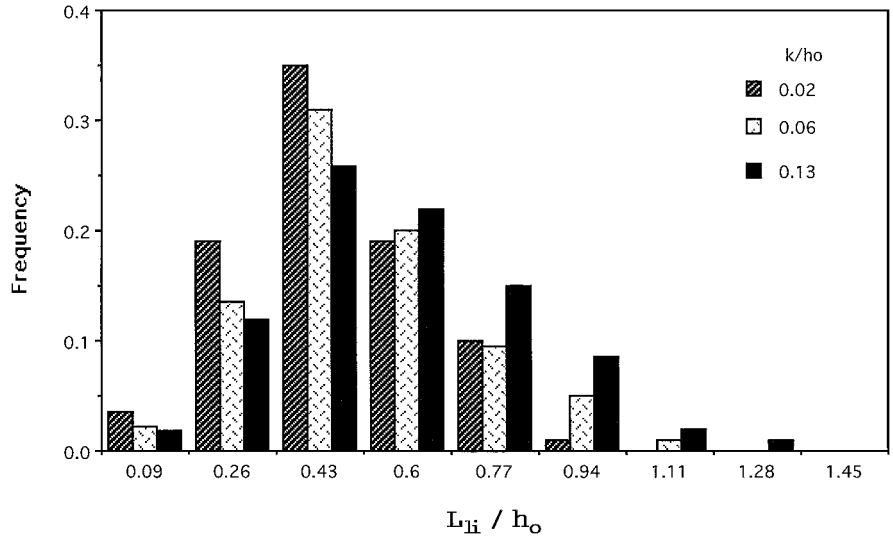

Fig. 25 Distribution of normalized ligament length as a function of relative roughness (*Fr* = 26 with 10% Polyox). Note that the ligament lengths are significantly smaller than those shown in Fig. 23.

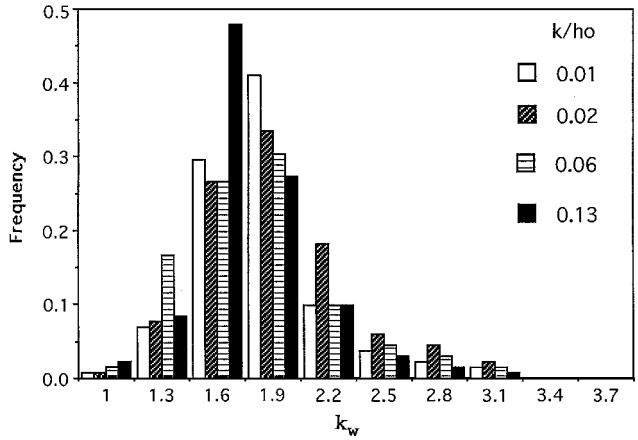

Fig. 26 Distribution of the disturbance wave number as a function of relative roughness (*Fr* = 26).

length, and smaller diameters than their drops (see Figs. 19 and 20 and 21 and 22). It is also seen that the length of the disturbance wave increases, as its diameter decreases toward the tip, giving the ligament the shape of a truncated cone. The angle α (see Fig. 11) of all of the recorded ligaments was measured. The mean angle of the ligaments leaning backward (as in Figs. 10 and 14) was found to be 81 $\pm$ 5 deg. Only rarely, some ligaments (about 3% of the total) leaned forward. Moreover, the change in α was about +4 deg from the inception of a ligament to its final stages (i.e., during its 200–300 ms existence). This suggests that there is very little or no apparent change in the mean angle of ligaments because the angle measurement is only accurate to within about $\pm$5 deg. The fact that the large majority of the ligaments lean backward is in conformity with the direction of the ejections. The Introduction notes that ejections occur in the second $(-u', +v')$ quadrant (Q2 event). They are violent upward and backward moving parcels of fluid of lower than average downstream velocity[33,34] and should lead to ligaments leaning mostly backward while moving forward with the stream. It is a well-known fact[32–36] that some ejections could occur, however rarely, in the first $(+u', +v')$ quadrant. These lead to forward leaning ligaments. They are relatively small and seldom give birth to drops.

It is possible to estimate the air resistance experienced by a ligament emerging from the jet through the use of the standard drag-force expression given by $F = 0.5 C_d \rho_a (h_0 U_0/\bar{h})^2 D_{li} L_{li}$. Assuming a ligament with $L_{li}/h_0 = 2.6$ (see Fig. 23) and $D_{li}/h_0 = 0.4$ (see Fig. 22), $C_d = 1.2$, $\rho_a = 1.22\,\text{kg/m}^3$, $h_0 = 5.8$ mm, $\bar{h}/h_0 = 1.7$ (see Fig. 17), and $U_0 = 6.2$ m/s, one has $F \approx 0.34$ g. The torque experienced by the ligament would be about 2.5 mm · g. Clearly, the doubling of the length or the diameter of the ligament, or the use of a larger drag coefficient, could not change the obvious conclusion that the external aerodynamics has no measurable effect on the spray formation.

The disturbance wave number k_w $(= \pi D_{li}/\lambda)$, just prior to drop pinch-off, was evaluated as accurately as possible. The individual wave numbers carry an uncertainty of about 20% because the determination of the wavelength λ requires more subjective interpretation than some of the other parameters. It is expected that this uncertainty is random in nature so that mean value calculations still provide reasonable estimates. Figure 26 shows that the wave number k_w displays a fairly constant mean value (about 1.80 with a standard deviation of 0.4) and a nearly Gaussian profile. As noted in the Introduction, Rayleigh[12] has shown that the maximum rate of growth of the axisymmetrical disturbances on a capillary jet occurs at a wave number of $k_w = 0.697$. The large difference between that found in the present investigation and that of Rayleigh is attributable in part to the fact that near the tip the maximum diameter of the ligament is about 75% smaller than the mean diameter of the ligament, the length of the wave is about 80% larger than the mean, and the shape of the amplified wave is more like an elongated ellipsoid. The use of the values prevailing near the tip leads to a wave number of about 0.75, which is closer to that expected for the capillary jets. However, it is not our intention to assert that the wave number for a ligament should be identical to that predicted by Rayleigh. The disturbances in Rayleigh's analysis are infinitesimal, whereas those on ligaments are highly amplified. Furthermore, a ligament is more like a truncated cone rather than a circular capillary jet.

Ejections and Tip Velocities

It is evident from what has been presented so far that the internal flow structure of the liquid wall jet discharging into quiescent air is not the same as either a typical boundary layer or a submerged wall jet (e.g., air-into-air). The velocity profile in the latter is largely influenced by the strong shear at the periphery of the jet. Open-channel flows are well described by classical boundary-layer analyses near the wall, and the relatively docile free surface variations caused by slowly rising boils and kolks[63] do not compare to the violent ejections observed in high-speed liquid wall jets.

The DPIV measurements have shown some striking differences between the internal structure of liquid wall jets and other boundary-layer flows. Figure 27 shows a representative plot of $\langle v' \rangle$ for $k/h_0 = 0.06$ and $Fr = 26$. Clearly, $\langle v' \rangle$ increases near the free surface, whereas it decreases rapidly with distance from the wall in ordinary wall jets or boundary layers[43] (Fig. 28). Furthermore, $\langle v' \rangle$

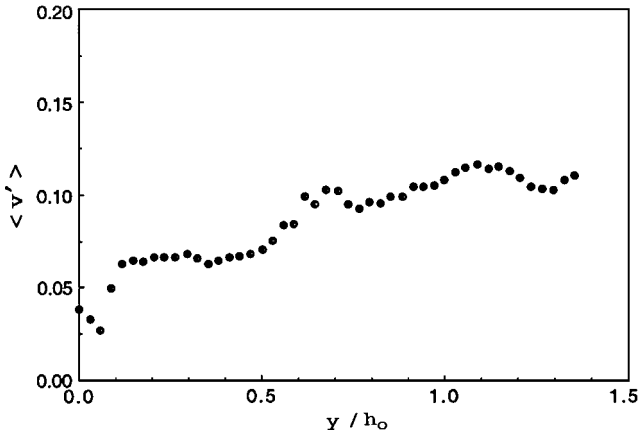

Fig. 27 Normalized rms value of the vertical component of velocity fluctuations (present study) ($k_0/h_0 = 0.06$).

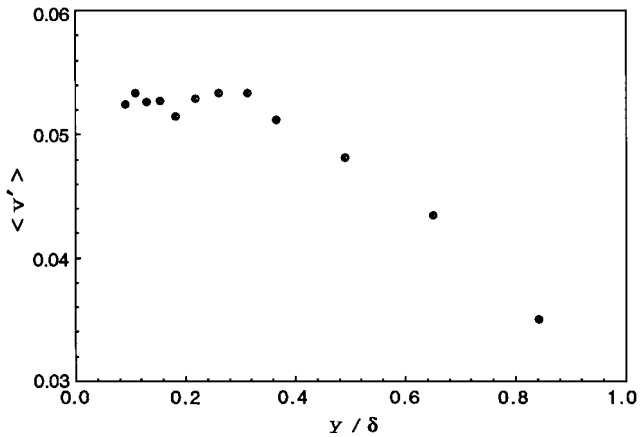

Fig. 28 Normalized rms value of the vertical component of velocity fluctuations in a boundary layer over a roughened surface (from Pimenta et al.[43] ($k_0/\delta = 0.06$).

in Fig. 27 is about twice as large as that in Fig. 28. The measurements of Nezu and Nakagawa,[63] in a rough-walled open- channel flow, yielded a maximum value closer to $\langle v' \rangle \approx 0.08$ as compared to $\langle v' \rangle \approx 0.055$ in Fig. 28. The obvious conclusion is that the rise and demise of the free-surface structures are a consequence of the condition of the wall (here roughness) and the mutual interaction between the resulting flowfield and the free surface. Thus, the ejection of the ligaments must necessarily be controlled by the dynamics of the flowfield.

Figure 29 shows representative plots of the v component of velocity (as acquired with DPIV at three different times) for the case of $k/h_0 = 0.06$ and $Fr = 26$. The white areas indicate $v/U_0 < 0.10$, while the black areas show $v/U_0 > 0.10$. The circled regions show focused areas with upward velocities as large as large $v/U_0 \approx 0.2$. In view of this finding, the tip velocities of all ligaments, which eventually gave rise to one or more drops, were evaluated from the Lagrangian measurements, using only the images taken after the initial acceleration period of 5–10 ms. The results are shown in Fig. 30 for only $k/h_0 = 0.06$ and $Fr = 26$. The other wall roughnesses gave similar results. The cases of $k/h_0 = 0.01$ and 0.02 yielded about 32% smaller v/U_0 values, whereas the case of $k/h_0 = 0.13$ yielded 15% larger v/U_0. The most striking feature of these plots was the presence of two significantly different frequencies: a low tip-velocity range at high frequencies and a distinct high tip-velocity range at low frequencies.

The foregoing measurements strongly suggest that the ejections can be roughly divided into two groups: those resulting from the focusing effects (formation of high-pressure, high velocity regions) first noted by Peregrine,[37] and those resulting from nonfocused or regular turbulent events. In either case, the intensity of the fluctuations is enhanced by the retarded nature of the flow. As noted earlier,

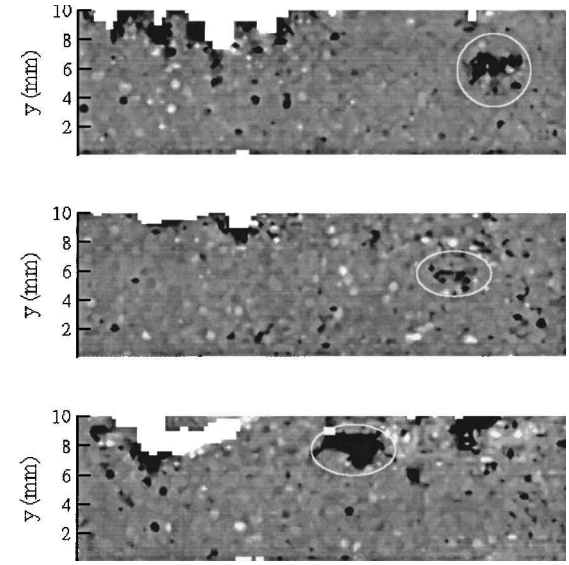

Fig. 29 Contour plots of velocity in the ligament formation region ($Fr = 26$) as acquired with DPIV. The white shades indicate $v/U_0 < 0.1$, while black shades indicate $v/U_0 > 0.1$. The encircled areas show the focused regions of high velocity ($k_0/h_0 = 0.06$).

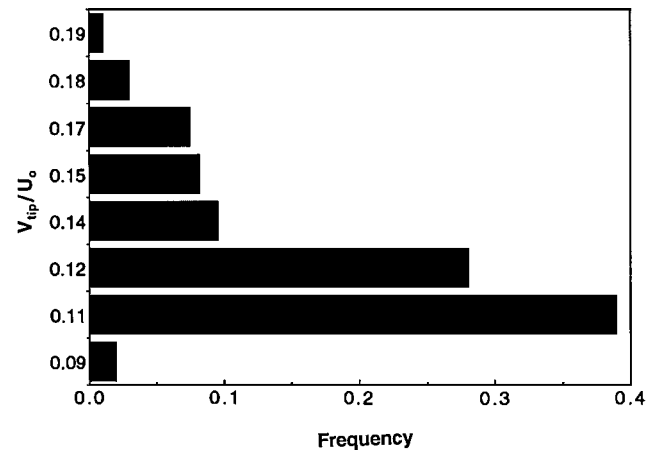

Fig. 30 Frequency distribution of the vertical component of the normalized tip velocity ($Fr = 26$, $k_0/h_0 = 0.06$).

van Oudheusden,[40] has shown that in retarded boundary layers the fluctuation levels in a large part of the boundary layer are significantly larger than in a fully developed turbulent boundary layer. A comparison of Figs. 23 and 30 suggests that the ligament lengths shown in Fig. 23 (e.g., for $k/h_0 = 0.06$) can be categorized into three groups: 1) L_{li}/h_0 smaller than about 1.2, resulting from relatively small, low-frequency, regular ejections; 2) L_{li}/h_0 larger than 1.2 and smaller than about 3, resulting from fairly strong regular ejections; and 3) L_{li}/h_0 larger than about 3, resulting from focused ejections at smaller frequencies. As also seen in Fig. 30, some low-frequency ejections are regular, and some are focused. In the light of the foregoing, Figs. 21–23 show that the focused ejections lead to taller and more slender ligaments, which give birth to larger drops.

The mechanism that emerges from our observations and measurements and from previous research on turbulent boundary layers can be summarized as follows. The form drag of individual roughness elements serves as an effective arrest mechanism and increases $\langle v' \rangle$ throughout the jet, renders the entire flow three-dimensional (not only near the wall, as in the case of confined or semi-infinite boundary-layer flows), forms a passive reservoir of low momentum fluid which is drawn on during ejection phases,[34,35] renders the entrainment extremely violent, with ejected fluid rising almost vertically from between the interstices of the roughness elements. The ejections, which are strong enough to reach the free surface, give rise to ligaments and drops whose number and intensity increase

with increasing roughness and jet speed. More interestingly, however, dynamic processes[37] (not yet sufficiently understood) cause the formation of high-velocity and -pressure regions in liquids by focusing effects. These, combined with the consequences of the flow retardation,[40] lead to focused ejections, which emerge as long and slender filaments.

Conclusions

Despite the wealth of statistical information based on mean values of drops, no prior work sought to investigate the characteristics of ligaments and drops and the structure of flow beneath the free surface of a turbulent plane liquid wall jet discharging into quiescent air. This investigation was focused on the surface structures in the region of ligament forest and drop formation in order to elucidate the characteristics of the free-surface structures in high-speed liquid wall jets, to explain, to the extent possible, the physics behind the observed behavior by qualifying and quantifying the influence of the dominant factors such as relative wall roughness and Froude number in a narrow range of Weber numbers, and to relate the subsurface nature of the jet to that of its free surface

Using flow visualization, DPIV, Optimus-MA software, and Eulerian and Lagrangian measurements, the length and diameter of ligaments, the length of the Rayleigh waves, the velocity of the tip of ligaments, and the diameter of drops were quantified, and their frequency of occurrence was evaluated using as many as 8800 evaluations by two independent researchers, mostly at a Froude number of 26. The DPIV measurements within the jet helped to identify focused regions of high velocity. These, coupled with turbulence measurements and tip velocities, helped to explain the reason for the occurrence of very long and slender ligaments. The ejections were then classified into two groups: the normal ejections and the focused ejections. The following are the additional conclusions drawn from this work:

1) A liquid wall jet discharging into quiescent air is unlike the commonly known wall jet (fluid into same fluid) and boundary-layer flows. The velocity and turbulence structures are strongly affected by the condition of the wall and by the structures on the free surface.

2) The ligaments lean mostly backward while moving forward with the stream because the majority of the ejections occur, as in boundary-layer flows, in the second $(-u', +v')$ quadrant.

3) It has been demonstrated in as many ways as possible that the aerodynamic effects on free-surface structures are negligible.

4) Wall roughness has a significant effect on the size and frequency distribution of ligaments and drops. At lower jet velocities and smaller wall roughnesses the distributions of relative length and diameter of ligaments tend to skew toward smaller values.

5) Reductions in drop diameters and ligament diameters and lengths for a given roughness can be achieved most effectively by decreasing the Froude number. When the inverse is desirable (for certain industrial processes), it is necessary to use thinner jets with larger velocities. This is so because the thinner the jet the stronger the interaction between the wall and the free surface and the resulting turbulence.

6) Detailed processing of data at larger Weber and Froude numbers from a spray prediction and numerical simulation point of view is underway and will be reported in the future.

Acknowledgments

This investigation has been supported by the Office of Naval Research (ONR; Code 333). We are particularly indebted to Edwin P. Rood and L. Patrick Purtell for their support and encouragement during their tenures as the program director at ONR. The assistance with the experiments and data evaluation of A. G. Salinas and R. Vaidyanathan is greatly appreciated.

References

[1]Lefebvre, A. H., *Atomization and Sprays*, Hemisphere, New York, 1989.

[2]Middleman, S., *Modeling Axisymmetric Flows—Dyamics of Films, Jets, and Drops*, Academic Press, New York, 1995.

[3]Kuo, K. K., *Recent Advances in Spray Combustion: Spray Atomization and Drop Burning Phenomena*, Vol. 1, AIAA, Reston, VA, 1996, p. 517.

[4]Crowe, C., Sommerfeld, M., and Tsuji, Y., *Multiphase Flows with Droplets and Particles*, CRC Press, Boca Raton, FL, 1998.

[5]Sirignano, W. A., *Fluid Dynamics and Transport of Droplets and Sprays*, Cambridge Univ. Press, New York, 1999.

[6]Hoyt, J. W., and Taylor, J. J., "Waves on Water Jets," *Journal of Fluid Mechanics*, Vol. 88, Pt. 1, 1977, pp. 119–123.

[7]Hoyt, J. W., and Taylor, J. J., "Turbulence Structure in a Water Jet Discharging in Air," *Physics of Fluids*, Vol. 20, Pt. 2, No. 10, 1977, pp. S253–S257.

[8]Hoyt, J. W., and Taylor, J. J., "Effect of Nozzle Boundary Layer on Water Jets Discharging in Air," *Jets and Cavities* edited by J. H. Kim, O. Furuya, and B. R. Parkin, Vol. 31, American Society of Mechanical Engineers, New York, 1985, pp. 93–100.

[9]Dai, Z., Hsiang, L.-P., and Faeth, G. M., "Spray Generation at the Free Surface of Turbulent Bow Sheets," *Twenty-First Symposium on Naval Hydrodynamics*, National Academy Press, Washington, DC, 1997, pp. 490–505.

[10]Mayer, W. O. H., "Coaxial Atomization of a Round Jet in a High Speed Gas Stream: A Phenomenological Study," *Experiments in Fluids*, Vol. 16, 1994, pp. 401–410.

[11]Mayer, W. O. H., Schik, H. A., Vielle, B., Chauveau, C., Gökalp, I., Talley, D. G., and Woodward, R. D., "Atomization and Breakup of Cryogenic Propellants Under High-Pressure Subcritical and Supercritical Conditions," *Journal of Propulsion and Power*, Vol. 14, No. 5, 1998, pp. 835–842.

[12]Rayleigh, Lord, "On the Instability of Jets," *Proceedings of the London Mathematical Society*, Vol. 10, 1879, pp. 4–13 (as quoted in *Scientific Papers by Lord Rayleigh*, Dover, New York, 1945).

[13]Weber, C., "Zum Zerfall eines Flüssigkeitsstrahles," *Zeitschrift für Angewandte Mathematik und Mechanik*, Vol. 11, No. 2, 1931, pp. 136–154.

[14]Ohnesorge, W., "Formation of Drops by Nozzles and the Breakup of Liquid Jets," *Zeitschrift für Angewandte Mathematik und Mechanik*, Vol. 16, 1936, pp. 355–358.

[15]Squire, H. B., "Investigation of the Instability of a Moving Liquid Film," *British Journal of Applied Physics*, Vol. 4, 1953, pp. 167–169.

[16]Hagerty, W. W., and Shea, J. F., "A Study of the Stability of Plaine Fluid Sheets," *Journal of Applied Mechanics*, Vol. 22, Feb. 1955, pp. 418–422.

[17]Brown, D. R., "A Study of the Behaviour of a Thin Sheet of Moving Liquid," *Journal of Fluid Mechanics*, Vol. 10, Pt. 2, 1961, pp. 297–305.

[18]Luca, L. de., "Experimental Investigation of the Global Instability of Plane Sheet Flows," *Journal of Fluid Mechanics*, Vol. 399, Nov. 1999, pp. 355–376.

[19]Yakubenko, P. A., "Global Capillary Instability of an Inclined Jet," *Journal of Fluid Mechanics*, Vol. 346, Sept. 1997, pp. 181–200.

[20]Binnie, A. M., "Experiments on the Onset of Wave Formation on a Film of Water Flowing Down a Vertical Plane," *Journal of Fluid Mechanics*, Vol. 2, Pt. 6, 1957, pp. 551–553.

[21]Benjamin, T. B., "Wave Formation in Laminar Flow Down an Inclined Plane," *Journal of Fluid Mechanics*, Vol. 2, Pt. 6, 1957, pp. 554–574.

[22]Knuth, E. L., "The Mechanics of Film Cooling—Part I," *Jet Propulsion*, Vol. 24, 1959, pp. 359–610.

[23]Sarpkaya, T., and Neubert, D. E., "Interaction of a Streamwise Vortex with a Free Surface," *AIAA Journal*, Vol. 32, No. 3, 1994, pp. 594–600.

[24]van Rossum, J. J., "Experimental Investigation of Horizontal Liquid Films: Wave Formation, Atomization, Film Thickness," *Chemical Engineering Science*, Vol. 11, 1959, pp. 35–52.

[25]Finley, P. J., Khoo, C. P., and Chin, J. P., "Velocity Measurements in a Thin Turbulent Water Layer," *La Houille Blanche*, Vol. 21, May 1966, pp. 713–721.

[26]Phinney, R. E., "The Breakup of a Turbulent Jet in a Gaseous Atmosphere," *Journal of Fluid Mechanics*, Vol. 60, Pt. 4, 1973, pp. 689–701.

[27]McCarthy, M. J., and Malloy, N. A., "Review of Stability of Liquid Jets and the Influence of Nozzle Design," *Chemical Engineering Journal*, Vol. 7, No.1, 1974, pp. 1–20.

[28]Lin, S. P., and Reitz, R. D., "Drop and Spray Formation From a Liquid Jet," *Annual Review of Fluid Mechanics*, Vol. 30, 1998, pp. 85–105.

[29]Freund, J. B., Lele, S. K., and Moin, P., "Numerical Simulation of a Mach 1.92 Turbulent Jet and Its Sound Field," *AIAA Journal*, Vol. 38, No. 11, 2000, pp. 2023–2031.

[30]Robinson, S. K., and Kline, S. J., "Turbulent Boundary Layer Structure: Progress, Status and Challenges," *Structure of Turbulence and Drag Reduction*, edited by A. Gyr, Springer-Verlag, New York, 1990, pp. 3–32.

[31]Robinson, S. K., "Coherent Motions in the Turbulent Boundary Layer," *Annual Review of Fluid Mechanics*, Vol. 23, 1991, pp. 601–639; also, NASA TM 103859, 1991; also *Journal of Fluid Mechanics*, Vol. 412, June 1991, pp. 355–378.

[32]Demare, S., Labraga, L., and Tournier, C., "Comparison and Scaling of the Bursting Period in Rough and Smooth Walls Channel Flows," *Journal of Fluids Engineering*, Vol. 121, Dec. 1999, pp. 735–746.

[33]Grass, A. J., "Structural Features of Turbulent Flow over Smooth and Rough Boundaries," *Journal of Fluid Mechanics*, Vol. 50, Pt. 2, 1971, pp. 233–255.

[34]Raupach, M. R., "Conditional Statistics of Reynolds Stress in Rough-Wall and Smooth-Wall Turbulent Boundary Layers," *Journal of Fluid Mechanics*, Vol. 108, July 1981, pp. 363–382.

[35]Krogstad, P.-A., Antonia, R. A., and Browne, L. W. B., "Comparison Between Rough- and Smooth-Wall Turbulent Boundary Layers," *Journal of Fluid Mechanics*, Vol. 245, Dec. 1992, pp. 599–617.

[36]Bogard, D. G., and Tiederman, W. G., "Burst Detection with Single-Point Velocity Measurements," *Journal of Fluid Mechanics*, Vol. 162, Jan. 1986, pp. 389–413.

[37]Peregrine, D. H., "Presure on Breakwaters: A Forward Look," *Proceedings of the International Workshop on Wave Barriers in Deep Waters*, edited by T. Takayama, Port and Harbour Research Inst., Tokyo, 1994, pp. 553–573.

[38]Meier, G. E. A., Ehrenfried, K., Grabitz, G., and Rein, M., "Wave Models for Unsteady Separation and Jets," *Proceedings of Separated Flows and Jets, IUTAM Symposium*, edited by V. V. Kozlov, and A. V. Dovgal, Springer-Verlag, Berlin, 1991, pp. 503–512.

[39]Krogstad, P.-A., and Antonia, R. A., "Surface Roughness Effects in Turbulent Boundary Layers," *Experiments in Fluids*, Vol. 27, 1999, pp. 450–460.

[40]van Oudheusden, B. W., "An Experimental Study of Transition and the Development of Turbulence in a Linearly Retarded Boundary-Layer Flow," *The Aeronautical Journal*, Nov. 1999, pp. 497–509.

[41]Antonia, R. A., and Luxton, R. E., "The Response of a Turbulent Boundary Layer to a Step Change in Surface Roughness, Part 1. Smooth to Rough," *Journal of Fluid Mechanics*, Vol. 48, Pt. 4, 1971, pp. 721–761.

[42]Andreopoulos, J., and Wood, D. H., "The Response of a Turbulent Boundary Layer to a Short Length of Surface Roughness," *Journal of Fluid Mechanics*, Vol. 118, May 1982, pp. 143–164.

[43]Pimenta, M. M., Moffat, R. J., and Kays, W. M., "Turbulent Boundary Layer: An Experimental Study of the Transport of Momentum and Heat with the Effect of Roughness," Thermosciences Div., Dept. of Mechanical Engineering, Report HTM-21, Stanford Univ., Stanford, CA, June 1975.

[44]Gibbings, J. C., and Al-Shukr, S. M., "Effect of Sandpaper Roughness and Stream Turbulence on the Laminar Layer and its Transition," *Aeronautical Journal*, Vol. 101, Jan. 1997, pp. 17–24.

[45]Rein, M., "Turbulent Open-Channel Flows: Drop-Generation and Self-Aeration," *Journal of Hydraulic Engineering*, Vol. 124, Jan. 1998, pp. 98–102.

[46]Sarpkaya, T., "Vorticity, Free Surface, and Surfactants," *Annual Review of Fluid Mechanics*, Vol. 28, 1996, pp. 83–128.

[47]Sarpkaya, T., and Merrill, C. F., "Spray Formation at the Free Surface of Liquid Wall Jets," *Twenty-Second Symposium on Naval Hydrodynamics*, National Academy Press, Washington, DC, 1999, pp. 796–808.

[48]Buttler Ellis, M. C., Tuck, C. R., and Miller, P. C. H., "Dilute Emulsions and Their Effect on the Breakup of the Liquid Sheet Produced by Plat-Fan Spray Nozzles," *Atomization and Sprays*, Vol. 9, 1999, pp. 385–397.

[49]Sarpkaya, T., and Merrill, C. G., "High Speed Laser-PIV Imaging for the Eulerian-Lagrangian Measurement and Visualization of Spray on Wall-Bounded Jets," *Eighth International Conference on Liquid Atomization and Spray Systems*, CLASS, Pittsburgh, PA, 2000, pp. 1–8 (CD-ROM).

[50]Sarpkaya, T., "In-Line and Transverse Forces on Cylinders in Oscillatory Flow at High Reynolds Numbers," *Journal of Ship Research*, Vol. 21, No. 4, 1977, pp. 200–216.

[51]Sarpkaya, T., "Force on a Circular Cylinder in Viscous Oscillatory Flow at Low Keulegan-Carpenter Numbers," *Journal of Fluid Mechanics*, Vol. 165, April 1986, pp. 61–71.

[52]Dombrowski, N., and Fraser, R. P., "A Photographic Investigation into the Disintegration of Liquid Sheets," *Philosophical Transactions of the Royal Society of London*, Vol. 247, No. A924, 1954, pp. 101–130.

[53]Rouse, H., and Abol-Fetouh, A.-H., "Characteristics of Irrotational Flow Through Axially Symmetric Orifices," *Journal of Applied Mechanics*, Vol. 17, No. 2, 1950, pp. 421–426.

[54]Wickens, R. H., and Jeffreys, N. E., "The Use of the NRC/NAE Water Facilities in Canadian Aeronautical Research and Development," CPP-413, AGARD, 1986, pp. 7.1–7.19.

[55]Kline, S. J., and McClintock, F. A., "Describing Uncertainties in Single-Sample Experiments," *Mechanical Engineering*, Vol. 75, Jan. 1953, pp. 3–8.

[56]Moffat, R. J., "Contributions to the Theory of Single-Sample Uncertainty Analysis," *Journal of Fluids Engineering*, Vol. 104, No. 2, 1982, pp. 250–260.

[57]Schlichting, H., *Boundary-Layer Theory*, 7th ed., McGraw–Hill, New York, 1987, pp. 636–640.

[58]Davies, J. T., *Turbulence Phenomena*, Academic Press, New York, 1972, p. 115.

[59]van der Hegge-Zijnen, B. G., "Measurements of the Velocity Distribution in the Boundary Layer Along a Plane Surface," *Verhandelingen der Koninklijke Akademie van Wetenschappen te, Amsterdam*, Vol. 31, No. 5, 1928, p. 499.

[60]Volkart, P., "The Mechanism of Air Bubble Entrainment in Self-Aerated Flow," *International Journal of Multiphase Flow*, Vol. 6, 1980, pp. 411–423.

[61]Warholic, M. D., Massah, H., and Hanratty, T. J., "Influence of Drag-Reducing Polymers on Turbulence: Effects of Reynolds Number, Concentration and Mixing," *Experiments in Fluids*, Vol. 27, 1999, pp. 461–472.

[62]Sarpkaya, T., Rainey, P. G., and Kell, R. E., "Flow of Dilute Polymer Solutions About Circular Cylinders," *Journal of Fluid Mechanics*, Vol. 57, Pt. 1, 1973, pp. 177–208.

[63]Nezu, I., and Nakagawa, H., *Turbulence in Open Channel Flows*, A. A. Balkema Press, Rotterdam, The Netherlands, 1993, p. 420.

J. P. Gore
Associate Editor

Color reproductions courtesy of the Naval Postgraduate School.